The Glucagon-Like Peptide-1 Receptor Agonist Oxyntomodulin Enhances β-Cell Function but Does Not Inhibit Gastric Emptying in Mice

Adriano Maida, Julie A. Lovshin, Laurie L. Baggio, and Daniel J. Drucker

Mt. Sinai Hospital, Samuel Lunenfeld Research Institute, University of Toronto, Toronto, Ontario, Canada M5G 1X5

The proglucagon gene gives rise to multiple peptides that play diverse roles in the control of energy intake, gut motility, and nutrient disposal. Glucagon-like peptide-1 (GLP-1), a 30-amino-acid peptide regulates glucose homeostasis via control of insulin and glucagon secretion and by inhibition of gastric emptying and food intake. Oxyntomodulin (OXM) a 37-amino-acid peptide also derived from the proglucagon gene, binds to both the glucagon and GLP-1 receptor (GLP-1R); however, a separate OXM receptor has not yet been identified. Here we show that OXM, like other GLP-1R agonists, stimulates cAMP formation and lowers blood glucose after both oral and ip glucose administration, actions that require a functional GLP-1R. OXM also directly stimulates insulin secretion from murine islets and INS-1 cells in a glucose- and GLP-1R-dependent manner. Moreover, OXM ameliorates hyperglycemia and significantly reduces apoptosis in murine β-cells after streptozotocin administration and directly reduces apoptosis in thapsigargin-treated INS-1 cells. Unexpectedly, OXM, but not the GLP-1R agonist exendin-4, increased plasma levels of insulin after oral glucose administration. Moreover, OXM administered at doses that potently lower blood glucose had no effect on inhibition of gastric emptying but reduced food intake in WT mice. Taken together, these findings illustrate that although structurally distinct proglucagon-derived peptides such as GLP-1 and OXM engage the GLP-1R, OXM mimics some but not all of the actions of GLP-1R agonists *in vivo*. These findings may have implications for therapeutic efforts using OXM as a long-acting GLP-1R agonist for the treatment of metabolic disorders. (*Endocrinology* 149: 5670–5678, 2008)

FOOD INGESTION IS associated with activation of neural and hormonal mechanisms that regulate gastrointestinal motility and gastric, pancreatic, and biliary secretion, preparing the gastrointestinal mucosa for the digestion and absorption of incoming nutrients. A complex network of neural relay mechanisms receives signals from the gut and relays information to the central nervous system, which in turn contributes to the control of gut motility, satiety, and nutrient disposal. A second sophisticated network is comprised of gut endocrine cells distributed throughout the stomach and both proximal and distal gut mucosa. Enteroendocrine cells also play a critical role in the digestion and absorption of nutrients via the liberation of gut peptides that modify, at multiple levels, the integrated control of nutrient digestion, absorption, and energy assimilation.

Diversity of information derived from endocrine networks is achieved through multiple molecular mechanisms, including gene duplication, alternative RNA splicing, posttranslational prohormone processing, and evolution of multiple related G protein-coupled receptors that are capable of differentially recognizing signals from structurally related peptides. The proglucagon gene, expressed in the pancreas, brain, and gastrointestinal tract, exemplifies many of the mechanisms used for diversification of peptide hormone action. For example, gene duplication gives rise to multiple proglucagon genes with conserved peptide sequences that may be differentially expressed in specific tissues (1). Similarly, alternative RNA splicing of the proglucagon gene, as described in fish and lizards (2, 3), produces a different profile of proglucagon-derived peptides in the pancreas *vs.* the gut mucosa. However, in mammals, tissue-specific posttranslational processing of proglucagon is the most common mechanism used for generation of unique profiles of proglucagon-derived peptides in different tissues (4).

In the pancreas, 29-amino acid glucagon is the primary bioactive peptide liberated, with the majority of carboxyl-terminal sequences contained within an unprocessed major proglucagon fragment (5). In contrast, coexpression of prohormone convertase-1 and proglucagon in enteroendocrine L cells results in the liberation of glicentin, oxyntomodulin (OXM), several small intervening peptides, and two glucagon-like peptides, GLP-1 and GLP-2 (6). Although the actions of GLP-1 and GLP-2 have been extensively described (7), the biological activity of OXM and glicentin, proglucagon-derived peptides that also contain the glucagon amino acid sequence, remains poorly understood. Furthermore, separate receptors for glicentin and OXM have not yet been identified.

OXM, a 37-amino-acid peptide isolated from gut mucosal extracts, was originally shown to be more potent than glucagon in the inhibition of gastric acid secretion from oxyntic glands (8–10). Subsequent studies demonstrated that OXM was a weak agonist at the liver glucagon receptor and was

also capable of stimulating insulin, somatostatin, and glucagon secretion from the endocrine pancreas (11–13). OXM enhanced glucose clearance via stimulation of insulin secretion but had no independent effect on insulin action in mice (13). Moreover, iv administration of OXM also potently increased intestinal glucose uptake in the rat (14). Nevertheless, the specific molecular mechanisms mediating these diverse actions of OXM remained poorly understood.

OXM also regulates the control of food intake. Both central and peripheral administration of OXM produced satiety and weight loss in rodents (15–18), and subsequent studies demonstrated that OXM inhibits food intake and increases energy expenditure, leading to weight loss in human subjects (19). Although OXM interacts with both the glucagon and GLP-1 receptors (GLP-1R), experiments using the GLP-1R antagonist exendin(9–39) (Ex-9) and Glp1r$^{-/-}$ mice have demonstrated that the anorectic effect of OXM is mediated through the GLP-1R (17, 18). Remarkably, however, there is little information about whether OXM also exhibits GLP-1R-dependent actions important for control of glucoregulation. Accordingly, we have now examined whether OXM exerts a spectrum of glucoregulatory actions that require a functional GLP-1R.

Materials and Methods

Peptides and reagents

All peptides were reconstituted in either PBS or sterile water, aliquoted, and stored at −80 C. Exendin-4 (Ex-4) and Ex-9 were purchased from California Peptide Research Inc. (Napa, CA). OXM was purchased from Bachem (Torrance, CA) and Pepceuticals (Nottingham, UK). Tissue culture medium, fetal bovine serum (FBS), and G418 were purchased from Invitrogen (San Diego, CA). Acetaminophen (paracetamol), forskolin (FSK), 3-isobutyl-1-methylxanthine, thapsigargin (Tg), streptozotocin (STZ), collagenase V, Hanks' balanced salt solution (HBSS), and Histopaque were from Sigma Chemical Co. (St. Louis, MO).

Animal experiments

All animal experiments were carried out with strict adherence to the protocols and procedures outlined by the Toronto General Hospital and Mt. Sinai Hospital Animal Care Committees. Wild-type mice (C57BL/6) were purchased from Charles River Laboratories (Montreal, Quebec, Canada). Mice were allowed to acclimatize to the animal housing facilities at the Toronto General Hospital at least 1 wk before experimentation. After acclimatization, animals were handled daily and sham-injected with PBS once daily to further acclimatize the animals to experimental protocol. Glp1r$^{-/-}$ male mice on a C57BL/6 genetic background were used for these studies (20). All mice were 10–14 wk of age at the commencement of experiments and were maintained on a 12-h light, 12-h dark cycle and allowed *ad libitum* access to water and standard rodent chow, with exceptions as noted in the experimental protocols.

Oral and ip glucose tolerance tests and plasma insulin levels

Mice were fasted overnight and weighed, and blood glucose levels were measured by tail vein sampling using a handheld glucometer (Glucometer Elite Blood Glucose Meter; Bayer Inc., Toronto, Ontario, Canada). Mice were injected (ip) with PBS, Ex-4, or OXM (at various doses), and glucose was administered 5 min later (1.5 g/kg body weight) either via oral gavage [oral glucose tolerance test (OGTT)] or by ip injection [ip glucose tolerance test (IPGTT)]. Blood glucose levels were measured by tail vein sampling at 10, 20, 30, 60, 90, and 120 min after glucose administration. At the 10-min time point, a larger blood sample (100 μl) was collected from the tail vein and immediately mixed with 10 μl of a chilled solution containing 5000 kIU/ml Trasylol (Bayer), 32 mM EDTA, and 0.01 mM Diprotin A (Sigma Chemical Co., St. Louis, MO) and kept on ice. Plasma was obtained by centrifugation at 4 C and stored at

−80 C until determination of plasma insulin levels using LINCOplex multiplex ELISA (Millipore, Billerica, MA) as described (20). To obtain detailed profiles of glucose-stimulated insulin secretion by OXM and Ex-4, a separate experiment was performed where C57BL/6 male mice were injected (ip) with peptides/PBS 5 min before glucose administration (1.5 g/kg ip) and 50 μl blood aliquots collected from the tail vein into heparinized Microvette tubes (Sarstedt, Germany) at 0, 2, 5, 10, and 30 min after glucose administration. Plasma was separated as above and plasma insulin levels measured using an ultrasensitive mouse insulin ELISA (Alpco Diagnostics, Salem, NH).

Food intake studies

Mice were fasted in individual cages overnight (16 h) before food intake studies. Mice were weighed and injected with Ex-4 (1 μg), OXM (250 μg), or PBS. Mice were allowed *ad libitum* access to a premeasured amount of standard rodent chow with free access to water. Food intake was then measured at 1, 2, 4, 6, and 24 h.

Gastric emptying studies

Gastric emptying rate was assessed using two protocols. To measure solid-phase gastric emptying, mice were fasted in individual cages overnight (16 h) and then allowed *ad libitum* access to a premeasured amount of rodent chow for 1 h. Food intake was determined by reweighing the rodent chow after 1 h of refeeding. Mice were injected with PBS, Ex-4 (3 μg), or OXM (10, 100, or 250 μg), deprived of food for 4 h, and then euthanized by Somnotol (sodium pentobarbital solution; MTC Pharmaceuticals, Cambridge, Ontario, Canada) injection followed by cervical dislocation. The stomach was isolated and gastric contents retrieved and weighed. The gastric emptying rate was determined using the following calculation: gastric emptying rate (percent) = [1 − (stomach content wet weight/food intake)] × 100 as described (21). In the second protocol, liquid-phase gastric emptying was assessed using the paracetamol absorption test. This test is based on the principle that paracetamol absorption occurs completely in the small intestine, with negligible absorption in the stomach (22), and therefore the rate of gastric emptying is directly related to the appearance of paracetamol in the blood. Mice were fasted for 6 h beginning at 0700 h on the day of the experiment. Mice were injected with PBS, high-dose OXM (250 μg), or Ex-4 (1 μg) 10 min before (t = −10) oral administration of a solution containing paracetamol at a dose of 100 mg/kg. Tail vein blood (50 μl) was collected into heparinized tubes at 15, 30, and 60 min after paracetamol administration. Plasma was separated by centrifugation at 4 C and stored at −20 C until measurement of paracetamol levels using an enzymatic-spectrophotometric assay (Diagnostic Chemicals Ltd., Oxford, CT).

STZ studies

After a 5-h fast (0800–1300 h), C57BL/6 mice were injected with STZ at a dose of 40 mg/kg·d for 5 consecutive days as previously described (23). Nondiabetic control mice were injected with vehicle (0.1 M sodium citrate, pH 5). For testing the effect of OXM on STZ-induced diabetes, OXM (50 μg) or PBS was administered twice daily (0900 and 1800 h) commencing 4 d before STZ and continued for 4 d after STZ injections ceased. Control nondiabetic mice were administered vehicle only. This dose of OXM was chosen based on preliminary dose-response experiments demonstrating its efficacy in reducing blood glucose and stimulating insulin secretion in an OGTT. Random-fed blood glucose was measured via a tail vein blood sample at 1000 h every 2–3 d. Approximately 35 d after the last STZ injection, levels of blood glycosylated hemoglobin (HbA1c) were determined using the DCA 2000+ Analyzer (Bayer) using a volume of blood (5 μl) taken from the tail vein. Mice were killed by CO_2 asphyxiation, and a portion of the pancreas was removed for analysis of pancreatic insulin content. Because treatment with Ex-4 has been previously shown to reduce STZ-induced islet apoptosis (23), a separate cohort of C57BL/6 mice was randomized to receive twice-daily PBS, OXM (50 μg), or Ex-4 (2.3 μg) according to the STZ protocol above. These mice were killed by CO_2 asphyxiation within about 24 h after the last STZ injection, and their pancreata were removed, cut into approximately 10 pieces, fixed in neutral-buffered formalin for 48 h, and embedded in paraffin for histological analyses of apoptosis.

Immunostaining and quantification of islet cleaved caspase-3 in pancreas sections

Paraffin blocks were cut to obtain serial sections for insulin and cleaved caspase-3 staining, respectively, according to the following conditions. Insulin immunostaining was carried out using rabbit antiinsulin (1:30 dilution; Dako, Glostrup, Denmark) as primary antibody and biotinylated goat antirabbit (1:200 dilution; Vector Laboratories, Burlingame, CA) as secondary antibody. The sections were then incubated with horseradish peroxidase-conjugated Ultra Streptavidin (ID Labs Inc., London, Ontario, Canada) for 30 min, and color was developed with freshly prepared 3,3'-diaminobenzidine tetrahydrochloride (Dako) solution. For detection of cleaved caspase-3, sections were microwave pretreated in citrate buffer (pH 6) followed by overnight incubation with rabbit anti-cleaved caspase-3 (1:600 dilution; Cell Signaling Technology Inc., Danvers, MA) primary antibody. After secondary antibody treatment (as above), color development was achieved with freshly prepared NovaRed solution (Vector). Serial sections for insulin and cleaved caspase-3 were scanned using the Scanscope Imagescope system (Aperio Technologies, Vista, CA) at ×20 magnification (24). The digital images were analyzed with Scanscope software (Aperio Technologies), using the insulin-stained slides to locate and select islets on the serial section stained for cleaved caspase-3. The number of red pixels (indicative of cleaved caspase-3) within circled islets were summed using an optimized positive pixel count algorithm and normalized per total islet area (square millimeters) analyzed per mouse. Approximately 90 islets from each mouse pancreas were analyzed.

Pancreatic insulin content

Frozen pancreas fragments were homogenized for 30 sec in ice-cold acid-ethanol solution (0.18 M HCl, 70% ethanol). After overnight incubation at 4 C, homogenates were centrifuged at $1600 \times g$ for 15 min. The supernatant was collected and stored at −20 C. The pellet was homogenized once more in acid-ethanol, incubated for 2 h at 4 C, centrifuged as before, and supernatant collected. Insulin was determined in these extracts using the rat insulin RIA kit (Linco Research, St. Charles, MO) and normalized to protein content, as assessed by the Bradford protein assay (Hercules, CA).

Islet cell isolation and measurement of insulin secretion

After CO_2 euthanasia, pancreata from 14-wk-old male C57BL/6 mice were inflated via the pancreatic duct with collagenase type V (1 mg/ml in HBSS), excised, and digested at 37 C for 10–15 min. The resulting digest was washed twice with cold HBSS (containing 0.25% wt/vol BSA), and islets were separated using a Histopaque density gradient. The interface containing islets was removed, washed with HBSS plus BSA, and islets were resuspended in RPMI medium containing 10% FBS. After 2 h of incubation at 37 C, islets were handpicked into fresh medium and allowed to recover overnight. Islets with preserved architectural integrity were used for insulin secretion experiments. For insulin secretion, islets were preincubated in Krebs-Ringer buffer containing 0.2% BSA, 10 mM HEPES (pH 7.4), and 2.8 mM glucose for 45 min. Batches of 10 islets were distributed into tubes containing 0.5 ml Krebs-Ringer buffer at 2.8 or 16.7 mM glucose, with or without OXM or Ex-4 at the indicated concentrations. After incubation for 1 h at 37 C, secretion medium was collected and stored at −20 C for assessment of insulin secretion. Islet insulin content was extracted by transfer of islets to cold acid-ethanol solution (70% ethanol, 0.18 M HCl). Extracts were briefly sonicated (10 sec), and insulin was measured by RIA (Linco).

Analysis of cAMP

Baby hamster kidney (BHK) cells stably transfected with the rat GLP-1R (18) were propagated in DMEM supplemented with 5% FBS, 100 U/ml penicillin, 100 μg/ml streptomycin, and 0.05 mg/ml G418. For analysis of cAMP production, cells were grown to 80% confluency in 24-well plates in the absence of G418. Cells were rinsed with PBS and then incubated in fresh medium containing 100 μM 3-isobutyl-1-methylxanthine and PBS, OXM, or Ex-4 at 37 C for 10 min. Reactions were terminated by the addition ice-cold absolute ethanol, and cell extracts

were collected and stored at −80 C until measurement of cAMP using a cAMP RIA kit (Biomedical Technologies, Stoughton, MA) (18).

INS-1 cells and insulin secretion/apoptosis assays

INS-1 832/3 cells were a kind gift from Dr. Christopher Newgard (Duke University, Raleigh, NC) and cultured as described (25) in RPMI medium containing 11.1 mM glucose supplemented with 10% FBS, 100 U/ml penicillin, 100 μg/ml streptomycin, 10 mM/liter HEPES, 2 mM glutamine, 1 mM sodium pyruvate, and 50 μM β-mercaptoethanol. For insulin secretion experiments, cells were seeded in 24-well plates at a density of 500,000 cells per well and grown to confluence. Growth medium was replaced with RPMI containing 5 mM glucose (along with above indicated supplements) for approximately 16 h before insulin secretion assay. Insulin secretion was carried out as described (25). Briefly, cells were rinsed once in HEPES balanced salt solution (HEBSS) containing 3 mM glucose and subsequently preincubated for 2 h at 37 C in the same medium. Cells were then treated with HEBSS containing 3 mM glucose or 15 mM glucose with or without peptides at the indicated concentrations and incubated at 37 C for an additional 2 h. Secreted insulin levels were quantified by RIA (Linco) and corrected for cellular protein content as measured using the Bradford protein assay (Bio-Rad) with BSA as a standard. For apoptosis assays, cells were seeded in 24-well plates at 200,000 cells per well approximately 48 h before assay. For the last 16 h of this period, the medium was changed to serum-free RPMI containing 3 mM glucose, 0.1% BSA, and routine concentrations of other medium supplements. On the day of the experiment, the latter medium was used to treat cells with OXM, Ex-4, OXM plus Ex-9, or FSK with or without Tg and incubated at 37 C for 6 h. FSK and Tg stocks were prepared in dimethylsulfoxide, and final concentrations of this vehicle were equal in all treatment groups. Apoptosis in cells was quantified using the Cell Death ELISA[PLUS] (Roche, Indianapolis, IN), which quantifies levels of cytoplasmic nucleosomes, a late marker of apoptosis. Absorbance was measured at 405 nm with 492 nm as a reference, and values are expressed relative to control (untreated) cells.

Statistical analysis

All data are presented as means ± SEM. Statistical significance was determined by unpaired *t* tests or one- or two-way ANOVA and Bonferroni's or Dunnett's *post hoc* test as applicable. All statistical analysis was performed using GraphPad Prism version 4.02 software (GraphPad Software Inc., San Diego, CA). A *P* value <0.05 indicated a statistically significant difference.

Results

OGTT and IPGTT studies

To study the effect of OXM on glycemic excursion, we administered glucose either by the oral or ip route, with or without concomitant administration of OXM (1–50 μg) to wild-type mice. OXM dose-dependently reduced glycemic excursion after oral glucose challenge (Fig. 1, A and B), with the 10- and 50-μg doses reducing glucose to levels comparable to those achieved with a much lower dose of Ex-4 (100 ng). Analysis of plasma insulin levels 10 min after oral glucose administration demonstrated a significant increase in circulating insulin levels with doses of OXM (10 and 50 μg) that reduced glycemic excursion. In contrast, Ex-4 did not significantly increase plasma insulin levels during the OGTT, despite marked reduction of glycemic excursion in the same experiment (Fig. 1, A and C). Administration of OXM also reduced glycemic excursion after ip glucose challenge (Fig. 1, D and E).

To explore in more detail the differential insulinotropic response to OXM *vs.* Ex-4 after glucose challenge in the absence of confounding changes in gastric emptying, we analyzed plasma insulin levels after ip glucose challenge (Fig. 1F). Doses of Ex-4 and OXM that produced similar glucose-lowering efficacies (Fig. 1, D and E) resulted in dif-
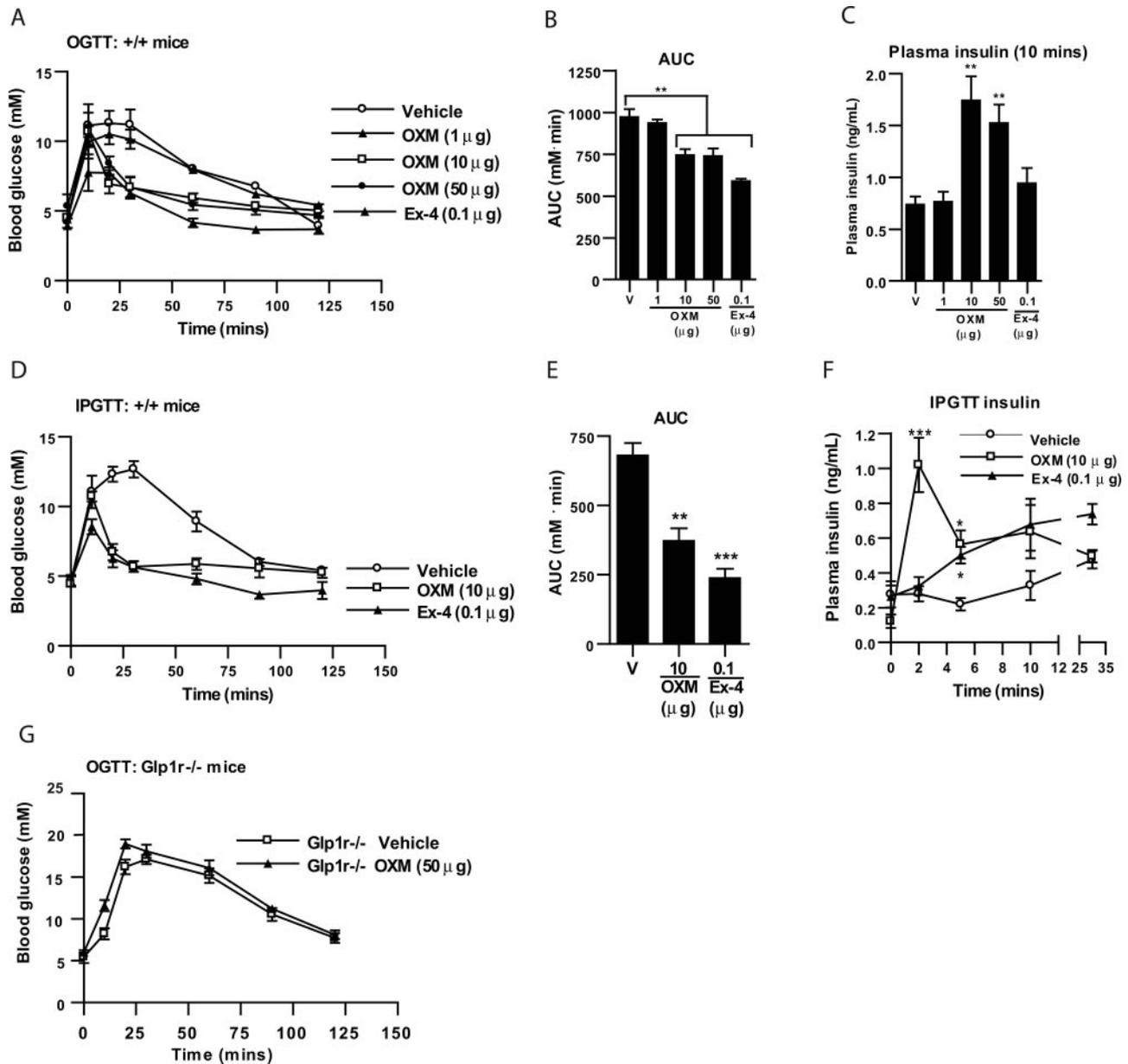
FIG. 1. OXM improves glucose tolerance and stimulates insulin secretion in wild-type mice but not in Glp1r$^{-/-}$ mice. Blood glucose values (A) with respective area under the curve (AUC) analysis (B) for an OGTT in overnight fasted C57BL/6$^{+/+}$ mice. Mice were injected ip with vehicle (V, PBS), OXM (1, 10, or 50 μg), or Ex-4 (0.1 μg) 5 min before oral glucose administration at time zero (n = 4). Plasma insulin (C) was measured at the 10-min time point for the OGTT (n = 7–12). Blood glucose values (D) with respective AUC analysis (E) and plasma insulin profile (F) for an IPGTT conducted 5 min after ip administration of OXM or Ex-4. To determine whether 50 μg OXM, which improved glucose tolerance and increased plasma insulin in wild-type mice, could improve glucose tolerance in mice lacking GLP-1Rs, an OGTT was performed in age-matched Glp1r$^{-/-}$ mice (G) given vehicle or OXM 5 min before glucose (n = 4–5 mice). *, $P < 0.05$; **, $P < 0.01$; ***, $P < 0.001$ *vs.* vehicle (V) group.

ferent insulin secretion profiles, with OXM stimulating a rapid peak in plasma insulin levels by 2 min, which subsequently dropped but remained significantly elevated after 5 min (Fig. 1F). In contrast, mice administered Ex-4 did not exhibit a robust rise in levels of plasma insulin at 2 min, although insulin levels were significantly higher in mice given Ex-4 compared with mice receiving glucose alone at 5 min (Fig. 1F). To determine whether the glucoregulatory actions of OXM were mediated through the known GLP-1R, we assessed whether OXM administration lowered glucose

in Glp1r$^{-/-}$ mice. The ability of OXM to lower glycemic excursion after oral glucose challenge was completely eliminated in Glp1r$^{-/-}$ mice (Fig. 1G).

Insulin secretion studies in murine islets and rat INS-1 β-cells

The available evidence suggests that GLP-1R agonists are capable of increasing insulin secretion through indirect neural pathways (26, 27), and via direct activation of β-cell GLP-

FIG. 2. OXM stimulates glucose-dependent insulin secretion from wild-type pancreatic islets and a rat β-cell line. A, Murine islets were preincubated in Krebs-Ringer buffer for 45 min at 2.8 mM glucose at 37 C before being distributed in batches of 10 islets per condition to tubes containing 2.8, 11.1, or 16.7 mM glucose with or without OXM in the presence or absence of 1 μM Ex-9 for 1 h at 37 C. Levels of insulin in the secretion medium were normalized to levels of islet insulin content. Insulin content values averaged about 25 ng/islet. Data shown are representative of three independent experiments, each with three replicates per condition. *, $P < 0.05$; **, $P < 0.01$; ***, $P < 0.001$ *vs.* glucose-matched control islets. ‡, $P < 0.05$ for OXM alone *vs.* OXM plus Ex-9. B, Rat INS-1 832/3 cells were incubated for 2 h at 37 C with HEBSS containing 3 mM glucose or 15 mM glucose with or without Ex-4, Ex-9 (1 μM), or OXM at the indicated concentrations. Insulin levels in medium were quantified and corrected for cellular protein content. Data shown are representative of three independent experiments. **, $P < 0.01$; ***, $P < 0.001$ *vs.* control cells incubated at 15 mM glucose. ‡, $P < 0.05$ for cells treated with OXM *vs.* treatment with OXM and Ex-9.
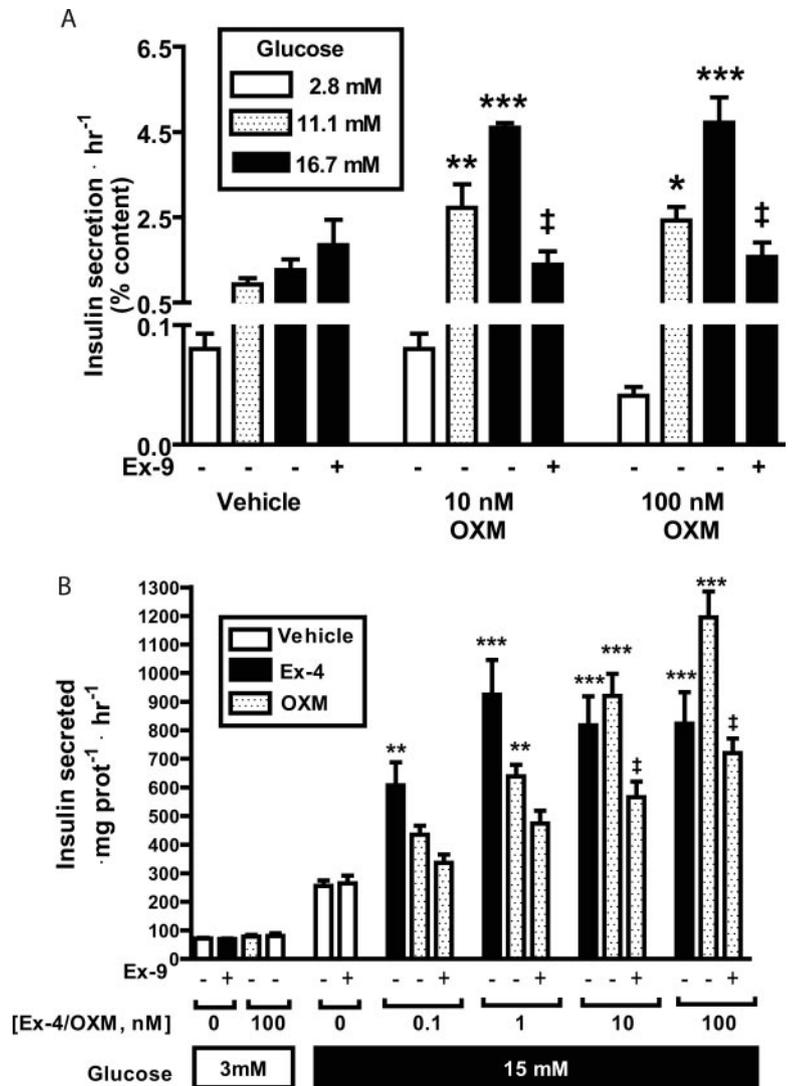
1Rs (26, 28). To determine whether OXM directly stimulates insulin secretion, we isolated islets from wild-type mice and assessed insulin secretion in the presence or absence of OXM or Ex-4. OXM had no effect on insulin secretion at low glucose (2.8 mM) concentrations but robustly stimulated insulin secretion in islets cultured in the presence of 11.1 or 16.7 mM glucose, with both 10- and 100-nM doses of OXM exhibiting similar potencies (Fig. 2A). Furthermore, the insulinotropic actions of OXM were significantly reduced in the presence of the GLP-1R antagonist Ex-9. OXM and Ex-4 also stimulated insulin secretion in glucose-responsive rat INS-1 cells (Fig. 2B), and the OXM-dependent potentiation of glucose-dependent insulin secretion was significantly attenuated in the presence of Ex-9.

β-Cell apoptosis

Considerable experimental evidence demonstrates that activation of GLP-1R signaling promotes resistance to apoptosis resulting in preservation of functional β-cell mass *in vivo* (23, 29, 30). To determine whether OXM is similarly capable of reducing β-cell apoptosis in an established murine model

of β-cell injury, we administered OXM to mice before and during administration of the β-cell toxin STZ according to the protocol depicted in Fig. 3A. Mice receiving OXM and STZ exhibited a 35% reduction in levels of activated caspase-3 within islets relative to STZ-treated mice treated with saline (Fig. 3, B and C). In a second cohort of mice, treatments with saline or OXM were administered before and during STZ as in Fig. 3A but continued for 4 additional days after the final STZ injection and random fed blood glucose levels were measured (Fig. 3D) periodically until d 40. Although random levels of glucose were similar between PBS- and OXM-treated mice, levels of HbA1c (Fig. 3F) were modestly but significantly reduced by OXM administration, and OXM-treated mice had significantly higher levels of pancreatic insulin content (Fig. 3G) detectable 30 days after the last injection of OXM.

To evaluate whether OXM was capable of directly reducing β-cell apoptosis in INS-1 832/3 β-cells, we assessed apoptosis in INS-1 832/3 β-cells via measurement of apoptosis-induced release of DNA-containing nucleosomes into the cytoplasmic compartment. Tg, a pharmacological inducer of endoplasmic retic-
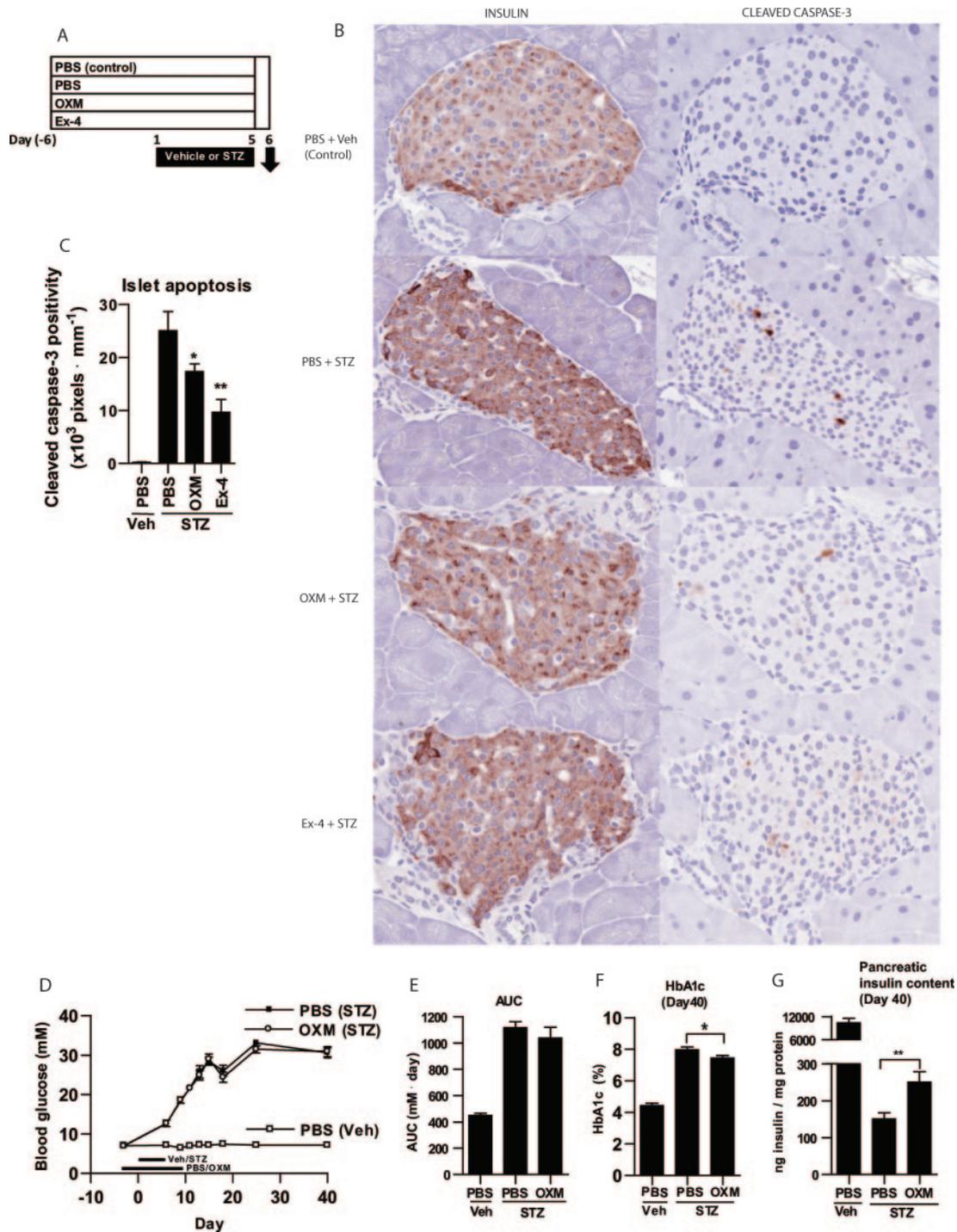
FIG. 3. OXM attenuates STZ-induced islet apoptosis and diabetes in mice. C57BL/6 mice were randomized into four groups as depicted in A: 1) control mice receiving saline treatments throughout (PBS) and sodium citrate buffer (pH 5) (Vehicle or Veh) for 5 d); 2) PBS and STZ, 3) 50 μg OXM twice daily plus STZ, or 4) 2.3 μg Ex-4 twice daily plus STZ. Injection of STZ (40 mg/kg) or vehicle was done once daily from d 1–5. Treatment with PBS or OXM or Ex-4 (twice daily) commenced 4 d before and throughout STZ administration. B, One cohort of mice was killed at d 6, 24 h after the last injection of STZ, for analysis of histology and histochemical detection of insulin and cleaved caspase-3 (magnification, ×400). C, Caspase-3 positivity within insulin-positive cells was quantified and corrected for total islet area (square millimeters) using an optimized pixel-counting algorithm together with Aperio Imagescope software. Approximately 90 islets per mouse were analyzed. n = 7–8 mice. *, $P < 0.05$; **, $P < 0.01$ *vs.* PBS-STZ mice. In a second experiment (D–G), mice were treated with PBS or OXM at doses indicated above, and peptide administration was continued for an additional 4 d after the final STZ injection and random fed blood glucose levels were measured (D) until d 40. Blood levels of HbA1c were measured (F) and pancreata procured for measurement of insulin content (G). n = 4–12. *, $P < 0.05$; **, $P < 0.01$. AUC, Area under the curve.
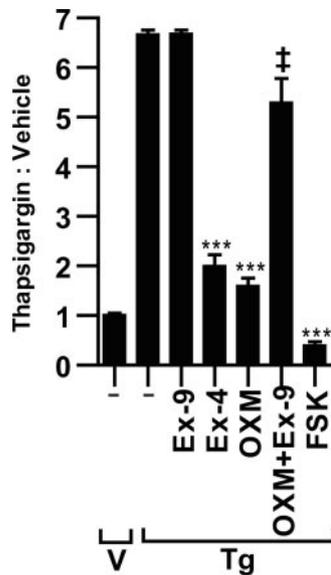
FIG. 4. OXM attenuates Tg-induced apoptosis in rat INS-1 β-cells in a GLP-1R-dependent manner. Cells were serum starved for 16 h (RPMI plus 0.1% BSA, 3 mM glucose) before being treated with fresh medium containing 0.5 μM Tg (V, dimethylsulfoxide) and one of the following: 1 μM Ex-9, 50 nM Ex-4, 50 nM OXM, 1 μM Ex-9 plus 50 nM OXM, or 10 μM FSK for 6 h. Data shown are representative of three independent experiments, each with three to four replicates. ***, $P < 0.001$ *vs.* Tg alone; ‡, $P < 0.001$ *vs.* OXM alone.

ulum stress and apoptosis in INS-1 cells (31, 32) caused a 6.5-fold increase in levels of cytoplasmic nucleosomes after 6 h (Fig. 4). In contrast, the levels of nucleosomes were markedly reduced by OXM and Ex-4 by 85 and 80%, respectively. Furthermore, Ex-9 reversed the protective effect of OXM in Tg-treated INS-1 cells, suggesting that OXM protects β-cells via a GLP-1R-dependent mechanism.

Gastric emptying and feeding studies

The results of the above studies demonstrate that OXM mimics some but not all of the glucoregulatory actions as-

cribed to GLP-1R agonists. Because OGTT (Fig. 1C) demonstrated that OXM, unlike Ex-4, significantly increased plasma insulin after oral glucose challenge, we hypothesized that OXM exerted reduced effects on gastric empting relative to the known inhibitory effects on gastric emptying demonstrated for GLP-1R agonists such as Ex-4. Gastric emptying in wild-type mice was measured using two techniques. In Fig. 5A, gastric emptying was calculated as the mass of wet stomach contents relative to the mass of food ingested in the presence of vehicle, OXM, or Ex-4. Although 3 μg Ex-4 potently inhibited gastric emptying rate, OXM used at doses up to 250 μg had no detectable effect on gastric emptying. Similarly, Ex-4, but not OXM, inhibited gastric emptying as assessed using the paracetamol absorption test (Fig. 5B) despite data illustrating that Ex-4 and OXM were both potent agonists at the GLP-1R *in vitro* (supplemental Fig. 1, published as supplemental data on The Endocrine Society's Journals Online web site at http://endo.endojournals.org). Because GLP-1R-dependent regulation of both gastric emptying and food intake is thought to require engagement of peripheral and central neural circuits, we next assessed the effects of acute ip administration of Ex-4 or OXM on food intake. Both OXM and Ex-4 significantly inhibited food intake (Fig. 5C), although the anorectic actions of Ex-4 were detectable for a more prolonged time period relative to the effects of OXM. Taken together, these observations reveal that OXM exhibits many but not all of the actions of GLP-1R agonists in mice *in vivo*.

Discussion

The concept that two distinct structurally related peptides modulate overlapping biological actions through a shared common receptor is not without precedent. For example, PTH and PTHrP compete for binding at the PTH receptor, and both proteins regulate bone resorption and calcium excretion (33). Similarly, although epidermal growth factor and TGF-α are encoded by distinct genes, both proteins are potent ligands for the epidermal growth factor receptor (34). Even more complexity is evident upon scrutiny of the mela-
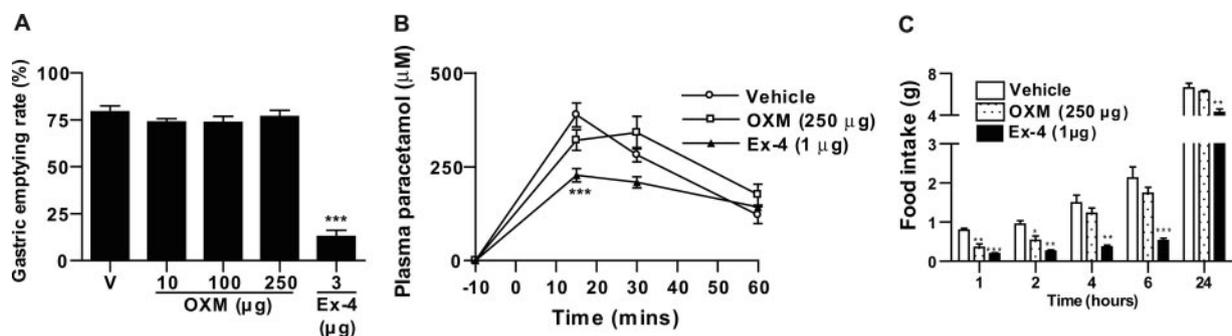

FIG. 5. Differential effects of OXM and Ex-4 on gastric emptying and food intake in C57BL/6 mice. Gastric emptying was assessed using two methods. A, Overnight fasted mice were allowed to refeed for 1 h and then were injected ip with vehicle (water, V), OXM at doses of 10, 100, or 250 μg, or Ex-4 (3 μg). Mice were killed 4 h later, stomach contents weighed, and gastric emptying calculated as described in *Materials and Methods*. n = 4–10. ***, $P < 0.001$ *vs.* vehicle-treated mice. B, Liquid-phase gastric emptying was assessed in 6-h fasted mice using the paracetamol absorption test. Vehicle (water), high-dose OXM (250 μg), or Ex-4 (1 μg) was administered by ip injection to 6-h fasted male mice 5 min before (t = −5) oral administration (t = 0) of a solution containing paracetamol at a dose of 100 mg/kg. Blood samples were taken from the tail vein before peptide administration (t = −10) and 15, 30, and 60 min after paracetamol administration. Plasma was separated by centrifugation and assayed for paracetamol. C, To determine whether OXM altered food intake, OXM (250 μg), Ex-4 (1 μg), or vehicle (water) was administered (ip) to overnight fasted mice and food intake monitored over 24 h. For B and C, n = 3–4. *, $P < 0.05$; **, $P < 0.01$; ***, $P < 0.001$, OXM or Ex-4 *vs.* vehicle-treated mice.

nocortin system, where peptides encoded by different genes, agouti and agouti-related peptide, compete with α-MSH for binding to melanocortin receptors (35). Much less common is the biological paradigm exemplified by OXM and GLP-1 wherein two peptides, derived from the same gene, are competitive ligands for a single common (GLP-1) receptor. Although it remains possible that OXM actions are modified by a separate as yet unidentified receptor or signaling protein, our data obtained using wild-type and receptor knockout mice convincingly demonstrate that the anorectic (18) and glucoregulatory actions of OXM require a functional GLP-1R.

Although multiple L cell-derived peptides secreted from the distal gut modulate food ingestion, the anorectic actions of PYY, GLP-1, and GLP-1R agonists such as Ex-4 have received the most attention due to their efficacy in human subjects. Both GLP-1 and Ex-4 bind to the central nervous system GLP-1R (36) and gain access to the central nervous system after peripheral administration (37). The inhibitory effects of GLP-1R agonists on feeding in mice requires a single GLP-1R (38) and likely involves direct and indirect regulation of satiety centers, inhibition of gastric emptying, and modulation of aversive signaling pathways (38–41). Indeed, repeated or continuous peripheral administration of GLP-1 or GLP-1R agonists such as Ex-4 or liraglutide to human subjects produces significant weight loss in clinical studies (42, 43). In contrast, there is much less information available about the chronic effects of OXM administration. However, a 4-wk trial of repeated OXM administration reduced food intake and body weight in association with increased energy expenditure in human subjects (19).

Although OXM inhibits food intake in fasted or fed rats (15–17), as well as in human subjects (19, 44), a separate receptor for OXM has not yet been identified. Hence, the precise receptor and signaling pathways transducing the anorectic and glucoregulatory actions of OXM remain uncertain. Our data clearly show that although OXM increases the levels of cAMP in BHK cells through either the GLP-1 or glucagon receptors (18), the glucoregulatory actions of OXM are mediated through a GLP-1R-dependent pathway.

An unexpected finding in our studies is the observation that OXM failed to inhibit gastric emptying *in vivo*. The GLP-1R-dependent control of gastric emptying likely involves neural regulation of gut motility and possibly direct interaction with gastric GLP-1Rs (45, 46). Moreover, the failure of OXM to inhibit gastric emptying in mice is even more surprising in that OXM is a partial glucagon receptor antagonist, and glucagon has been previously shown to inhibit gastric emptying in normal human subjects. In contrast to the lack of OXM action on gastric emptying in mice, administration of OXM to normal human subjects reduced basal and postprandial acid secretion and reduced the rate of gastric emptying together with a reduction in postprandial gut motility (47). Taken together, these divergent findings suggest that the actions of OXM are complex and may reflect species-specific interactions with one or more incompletely characterized OXM receptors.

Although OXM is capable of activating the glucagon receptor *in vitro*, our previous studies using Glp1r$^{-/-}$ mice clearly established that the anorectic effects of OXM require

a functional GLP-1R *in vivo* (18). Furthermore, our current data demonstrate that OXM fails to lower glucose in Glp1r$^{-/-}$ mice, consistent with an essential role for the GLP-1R in transducing the glucoregulatory actions of OXM *in vivo*. In contrast, although both OXM and GLP-1R agonists acutely increase heart rate and blood pressure in rodents *in vivo* (48–51), the chronotropic actions of GLP-1 require a functional GLP-1R (49, 52), whereas the ability of OXM to increase heart rate in mice occurs independently of the known GLP-1R (53). Furthermore, injection of GLP-1 or OXM produces differential patterns of neuronal activation in fasted mice *in vivo* (54), and OXM exerts differential activation of GLP-1R-dependent signal transduction in comparison with native GLP-1 *in vitro* (55). Taken together, our data demonstrate that OXM exhibits a partial spectrum of GLP-1R-dependent glucoregulatory actions *in vivo*, yet in contrast to the known effects of GLP-1R agonists on control of gut motility, OXM at the high doses used in our studies fails to inhibit gastric emptying in mice. These findings further refine our understanding of the GLP-1-like actions of OXM and emphasize the importance of understanding the mechanisms through which OXM exerts its glucoregulatory actions *in vivo*.

References

1. **Irwin DM** 2001 Molecular evolution of proglucagon. Regul Pept 98:1–12
2. **Irwin DM, Wong J** 1995 Trout and chicken proglucagon: alternative splicing generates mRNA transcripts encoding glucagon-like peptide 2. Mol Endocrinol 9:267–277
3. **Chen YE, Drucker DJ** 1997 Tissue-specific expression of unique mRNAs that encode proglucagon-derived peptides or exendin 4 in the lizard. J Biol Chem 272:4108–4115
4. **Mojsov S, Heinrich G, Wilson IB, Ravazzola M, Orci L, Habener JF** 1986 Preproglucagon gene expression in pancreas and intestine diversifies at the level of post-translational processing. J Biol Chem 261:11880–11889
5. **Patzelt C, Tager HS, Carroll RJ, Steiner DF** 1979 Identification and processing of proglucagon in pancreatic islets. Nature 282:260–266
6. **Dhanvantari S, Seidah NG, Brubaker PL** 1996 Role of prohormone convertases in the tissue-specific processing of proglucagon. Mol Endocrinol 10:342–355
7. **Drucker DJ** 2001 The glucagon-like peptides. Endocrinology 142:521–527
8. **Bataille D, Tatemoto K, Gespach C, Jornvall H, Rosselin G, Mutt V** 1982 Isolation of glucagon-37 (bioactive enteroglucagon/oxyntomodulin) from porcine jejuno-ileum. Characterization of the peptide. FEBS Lett 146:79–86
9. **Jarrousse C, Audousset-Puech MP, Dubrasquet M, Niel H, Martinez J, Bataille D** 1985 Oxyntomodulin (glucagon-37) and its C-terminal octapeptide inhibit gastric acid secretion. FEBS Lett 188:81–84

10. **Jarrousse C, Niel H, Audousset-Puech M-P, Martinez J, Bataille D** 1986 Oxyntomodulin and its C-terminal octapeptide inhibit liquid meal-stimulated acid secretion. Peptides 7:253–256

11. **Baldissera FG, Holst JJ, Knuhtsen S, Hilsted L, Nielsen OV** 1988 Oxyntomodulin (glicentin-(33–69)): pharmacokinetics, binding to liver cell membranes, effects on isolated perfused pig pancreas, and secretion from isolated perfused lower small intestine of pigs. Regul Pept 21:151–166

12. **Schjoldager BTG, Baldissera FG, Mortensen PE, Holst JJ, Christiansen J** 1988 Oxyntomodulin: a potential hormone from the distal gut. Pharmacokinetics and effects on gastric acid and insulin secretion in man. Eur J Clin Invest 18:499–503

13. **Parlevliet ET, Heijboer AC, Schroder-van der Elst JP, Havekes LM, Romijn JA, Pijl H, Corssmit EP** 2008 Oxyntomodulin ameliorates glucose intolerance in mice fed a high-fat diet. Am J Physiol Endocrinol Metab 294:E142–E147

14. **Collie NL, Zhu Z, Jordan S, Reeve Jr JR** 1997 Oxyntomodulin stimulates intestinal glucose uptake in rats. Gastroenterology 112:1961–1970

15. **Dakin CL, Gunn I, Small CJ, Edwards CM, Hay DL, Smith DM, Ghatei MA, Bloom SR** 2001 Oxyntomodulin inhibits food intake in the rat. Endocrinology 142:4244–4250

16. **Dakin CL, Small CJ, Park AJ, Seth A, Ghatei MA, Bloom SR** 2002 Repeated ICV administration of oxyntomodulin causes a greater reduction in body weight gain than in pair-fed rats. Am J Physiol Endocrinol Metab 283:E1173–E1177

17. **Dakin CL, Small CJ, Batterham RL, Neary NM, Cohen MA, Patterson M, Ghatei MA, Bloom SR** 2004 Peripheral oxyntomodulin reduces food intake and body weight gain in rats. Endocrinology 145:2687–2695

18. **Baggio LL, Huang Q, Brown TJ, Drucker DJ** 2004 Oxyntomodulin and glucagon-like peptide-1 differentially regulate murine food intake and energy expenditure. Gastroenterology 127:546–558

19. **Wynne K, Park AJ, Small CJ, Meeran K, Ghatei MA, Frost GS, Bloom SR** 2006 Oxyntomodulin increases energy expenditure in addition to decreasing energy intake in overweight and obese humans: a randomised controlled trial. Int J Obes (Lond) 30:1729–1736

20. **Hansotia T, Maida A, Flock G, Yamada Y, Tsukiyama K, Seino Y, Drucker DJ** 2007 Extrapancreatic incretin receptors modulate glucose homeostasis, body weight, and energy expenditure. J Clin Invest 117:143–152

21. **Baggio LL, Huang QH, Cao X, Drucker DJ** 2008 The long-acting albumin-exendin-4 GLP-1R agonist CJC-1134 engages central and peripheral mechanisms regulating glucose homeostasis. Gastroenterology 134:1137–1147

22. **Balkan B, Kwasnik L, Miserendino R, Holst JJ, Li X** 1999 Inhibition of dipeptidyl peptidase IV with NVP-DPP728 increases plasma GLP-1 (7–36 amide) concentrations and improves oral glucose tolerance in obese Zucker rats. Diabetologia 42:1324–1331

23. **Li Y, Hansotia T, Yusta B, Ris F, Halban PA, Drucker DJ** 2003 Glucagon-like peptide-1 receptor signaling modulates beta cell apoptosis. J Biol Chem 278:471–478

24. **Lamont BJ, Drucker DJ** 2008 Differential anti-diabetic efficacy of incretin agonists vs. DPP-4 inhibition in high fat fed mice. Diabetes 57:190–198

25. **Hohmeier HE, Mulder H, Chen G, Henkel-Rieger R, Prentki M, Newgard CB** 2000 Isolation of INS-1-derived cell lines with robust ATP-sensitive K^+ channel-dependent and -independent glucose-stimulated insulin secretion. Diabetes 49:424–430

26. **Ahren B** 2004 Sensory nerves contribute to insulin secretion by glucagon-like peptide-1 in mice. Am J Physiol Regul Integr Comp Physiol 286:R269–R272

27. **Vahl TP, Tauchi M, Durler TS, Elfers EE, Fernandes TM, Bitner RD, Ellis KS, Woods SC, Seeley RJ, Herman JP, D'Alessio DA** 2007 Glucagon-like peptide-1 (GLP-1) receptors expressed on nerve terminals in the portal vein mediate the effects of endogenous GLP-1 on glucose tolerance in rats. Endocrinology 148:4965–4973

28. **Drucker DJ, Philippe J, Mojsov S, Chick WL, Habener JF** 1987 Glucagon-like peptide I stimulates insulin gene expression and increases cyclic AMP levels in a rat islet cell line. Proc Natl Acad Sci USA 84:3434–3438

29. **Wang Q, Li L, Xu E, Wong V, Rhodes CJ, Brubaker PL** 2004 Glucagon-like peptide-1 regulates proliferation and apoptosis via activation of protein kinase B in pancreatic (INS-1) β-cells. Diabetologia 47:478–487

30. **Toyoda K, Okitsu T, Yamane S, Uonaga T, Liu X, Harada N, Uemoto S, Seino Y, Inagaki N** 2008 GLP-1 receptor signaling protects pancreatic β-cells in intraportal islet transplant by inhibiting apoptosis. Biochem Biophys Res Commun 367:793–798

31. **Yusta B, Baggio LL, Estall JE, Koehler JA, Holland DP, Li H, Pipeleers D, Ling Z, Drucker DJ** 2006 GLP-1 receptor activation improves β-cell function and survival following induction of endoplasmic reticulum stress. Cell Metabolism 4:391–406

32. **Yano T, Liu Z, Donovan J, Thomas MK, Habener JF** 2007 Stromal cell derived factor-1 (SDF-1)/CXCL12 attenuates diabetes in mice and promotes pancreatic β-cell survival by activation of the prosurvival kinase Akt. Diabetes 56:2946–2957

33. **Potts JT, Gardella TJ** 2007 Progress, paradox, and potential: parathyroid hormone research over five decades. Ann NY Acad Sci 1117:196–208

34. **Citri A, Yarden Y** 2006 EGF-ERBB signalling: towards the systems level. Nat Rev Mol Cell Biol 7:505–516

35. **Dinulescu DM, Cone RD** 2000 Agouti and agouti-related protein: analogies and contrasts. J Biol Chem 275:6695–6698

36. **Goke R, Larsen PJ, Mikkelsen JD, Sheikh SP** 1995 Distribution of GLP-1 binding sites in the rat brain: evidence that exendin-4 is a ligand of brain GLP-1 binding sites. Eur J Neurosci 7:2294–2300

37. **Kastin AJ, Akerstrom V** 2003 Entry of exendin-4 into brain is rapid but may be limited at high doses. Int J Obes Relat Metab Disord 27:313–318

38. **Scrocchi LA, Brown TJ, MacLusky N, Brubaker PL, Auerbach AB, Joyner AL, Drucker DJ** 1996 Glucose intolerance but normal satiety in mice with a null mutation in the glucagon-like peptide receptor gene. Nat Med 2:1254–1258

39. **Turton MD, O'Shea D, Gunn I, Beak SA, Edwards CMB, Meeran K, Choi SJ, Taylor GM, Heath MM, Lambert PD, Wilding JPH, Smith DM, Ghatei MA, Herbert J, Bloom SR** 1996 A role for glucagon-like peptide-1 in the central regulation of feeding. Nature 379:69–72

40. **Kinzig KP, D'Alessio DA, Seeley RJ** 2002 The diverse roles of specific GLP-1 receptors in the control of food intake and the response to visceral illness. J Neurosci 22:10470–10476

41. **Meier JJ, Gallwitz B, Schmidt WE, Nauck MA** 2002 Glucagon-like peptide 1 as a regulator of food intake and body weight: therapeutic perspectives. Eur J Pharmacol 440:269–279

42. **Drucker DJ** 2003 Enhancing incretin action for the treatment of type 2 diabetes. Diabetes Care 26:2929–2940

43. **Drucker DJ, Nauck MA** 2006 The incretin system: glucagon-like peptide-1 receptor agonists and dipeptidyl peptidase-4 inhibitors in type 2 diabetes. Lancet 368:1696–1705

44. **Cohen MA, Ellis SM, Le Roux CW, Batterham RL, Park A, Patterson M, Frost GS, Ghatei MA, Bloom SR** 2003 Oxyntomodulin suppresses appetite and reduces food intake in humans. J Clin Endocrinol Metab 88:4696–4701

45. **Imeryuz N, Yegen BC, Bozkurt A, Coskun T, Villanueva-Pennacarrillo ML, Ulusoy NB** 1997 Glucagon-like peptide-1 inhibits gastric emptying via vagal afferent-mediated central mechanisms. Am J Physiol 273:G920–G927

46. **Wettergren A, Wojdemann M, Holst JJ** 1998 Glucagon-like peptide-1 inhibits gastropancreatic function by inhibiting central parasympathetic outflow. Am J Physiol 275:G984–G992

47. **Schjoldager B, Mortensen PE, Myhre J, Christiansen J, Holst JJ** 1989 Oxyntomodulin from distal gut. Role in regulation of gastric and pancreatic functions. Dig Dis Sci 34:1411–1419

48. **Barragan JM, Rodriguez RE, Blazquez E** 1994 Changes in arterial blood pressure and heart rate induced by glucagon-like peptide-1-(7–36 amide) in rats. Am J Physiol 266:E459–E466

49. **Barragan JM, Rodriguez RE, Eng J, Blazquez E** 1996 Interactions of exendin-(9–39) with the effects of glucagon-like peptide-1-(7–36) amide and of exendin-4 on arterial blood pressure and heart rate in rats. Regulatory Peptides 67:63–68

50. **Yamamoto H, Lee CE, Marcus JN, Williams TD, Overton JM, Lopez ME, Hollenberg AN, Baggio L, Saper CB, Drucker DJ, Elmquist JK** 2002 Glucagon-like peptide-1 receptor stimulation increases blood pressure and heart rate and activates autonomic regulatory neurons. J Clin Invest 110:43–52

51. **Yamamoto H, Kishi T, Lee CE, Choi BJ, Fang H, Hollenberg AN, Drucker DJ, Elmquist JK** 2003 Glucagon-like peptide-1-responsive catecholamine neurons in the area postrema link peripheral glucagon-like peptide-1 with central autonomic control sites. J Neurosci 23:2939–2946

52. **Gros R, You X, Baggio LL, Kabir MG, Sadi AM, Mungrue IN, Parker TG, Huang Q, Drucker DJ, Husain M** 2003 Cardiac function in mice lacking the glucagon-like peptide-1 receptor. Endocrinology 144:2242–2252

53. **Sowden GL, Drucker DJ, Weinshenker D, Swoap SJ** 2007 Oxyntomodulin increases intrinsic heart rate in mice independent of the glucagon-like peptide-1 receptor. Am J Physiol Regul Integr Comp Physiol 292:R962–R970

54. **Chaudhri OB, Parkinson JR, Kuo YT, Druce MR, Herlihy AH, Bell JD, Dhillo WS, Stanley SA, Ghatei MA, Bloom SR** 2006 Differential hypothalamic neuronal activation after peripheral injection of GLP-1 and oxyntomodulin in mice detected by manganese-enhanced magnetic resonance imaging. Biochem Biophys Res Commun 350:298–306

55. **Jorgensen R, Kubale V, Vrecl M, Schwartz TW, Elling CE** 2007 Oxyntomodulin differentially affects glucagon-like peptide-1 receptor β-arrestin recruitment and signaling through $G\alpha_s$. J Pharmacol Exp Ther 322:148–154